JOURNAL OF MATERIALS SCIENCE **40** (2005) 77–85

Influence of composition and process parameters on the thermal spray deposition of UHMWPE coatings

Y. BAO
Department of Engineering Systems, London South Bank University, London, UK

T. ZHANG
School of Engineering, Kingston University, London, UK

D. T. GAWNE
Department of Engineering Systems, London South Bank University, London, UK

Ultra-high molecular weight polyethylene (UHMWPE) has remarkable properties in the bulk state and has substantial potential for use as a protective coating on metals. However, the molecular architecture responsible for these exceptional properties also causes difficulties in the formation of coatings by thermal spraying. This paper studies the effect of molecular weight, particle size and the influence of the addition of low-molecular weight binders on the structure and properties of combustion flame sprayed coatings. The flow of splats for each UHMWPE polymer and blends of selected polyethylenes was characterized by microstructural analysis and the performance of the resulting coatings evaluated by mechanical testing. A computational model was developed to calculate the temperature profiles of in-flight particles and to simulate the behaviour of particles during deposition. The model was applied to the polyethylene system and the experimental results show that the composition, the particle size and the process parameters are important factors in the optimization of coating quality.

1. Introduction

UHMWPE in the bulk state is established as a wear resistant polymer with a moderate coefficient of friction against steel counterfaces [1]. A large number of research studies have been published recently [1–9] covering the various aspects of the friction and wear behavior of bulk UHMWPE under various conditions. In spite of its high level of mechanical properties and wear performance, the application of UHMWPE is restricted owing to poor processability due to its high viscosity.

The high strength of UHMWPE makes it an attractive candidate for combined wear and corrosion-resistant coatings on metal components. The high cost of the material should not be an excessive burden because of the relatively small amounts needed for coatings. This paper explores the possibility of producing surface coatings from UHMWPE by thermal spraying. Thermal spraying consists of injecting powder particles into a hot jet in which they melt and are projected onto a substrate to form a coating. The particles flatten on impact with the substrate surface and rapidly solidify on top of one another to produce a deposit built up from innumerable splats. The spray gun is scanned over the substrate until a coating of the required thickness is achieved. An important requirement of the process is that the powder particles flow extensively on impact with substrate. This enables them to make close contact with the irregularities of the underlying substrate surface and form dense coatings. It is unknown whether or not the high viscosity of UHMWPE will adversely affect particle flow and the quality of the coatings. Experimental trials were undertaken with a series of polyethylenes with relative molecular weights up to 6 million. The resulting coatings were characterized and a computational model developed to simulate and optimize the process.

2. Experimental details

Four polymer powders were used in this study: two ultrahigh molecular weight polyethylenes (UHMWPE), ethylene acrylic acid (EAA) and UHMWPE-EAA composite powder. The details of these powders are given in Table I. The substrate used for adhesion test was plain carbon steel. The coatings were deposited by combustion flame spraying using acetylene as the fuel gas and compressed air as the oxidant.

A direct pull-off technique which conforms to ASTM D4541 and BS 3900-E10 was used to measure the adhesion of the deposits to steel. The measurement was performed using an Instron tensile machine: a steel cylinder 20 mm in diameter was adhesively bonded to the coating using Araldite 2015 and the tensile force

TABLE I Polymer powders and their physical properties

Powder	Particle size (μm)	Melting temperature (°C)	Molecular weight (g mol^{-1})	Density (Mg m^{-3})
A UHMWPE	D_{50}: 27 μ D_{90}: 50 μ	136	6 000 000	0.93
B UHMWPE	D_{50}: 120 μ D_{90}: 156 μ	130–153	2 000 000	0.94
EAA (6.5% ac)	D_{90}: 116 D_{50}: 68	80–100		0.91–0.97
UHMWPE-EAA	D_{50}: 108 μ D_{90}: 151 μ			

required to detach the coating from the substrate was measured. The crosshead speed used in the tests was 5 mm/min. The polymer coating surfaces were roughened with silicon carbide paper and the test cylinder was grit blasted before applying the adhesive in order to maximize the strength of the adhesive joint.

Bend tests were carried out to assess the resistance of the coatings to cracking and/or detachment from a metal substrate when subjected to bending conditions. This provides information on a flexibility and adhesion of the coatings to the steel substrate. The coatings were deposited on a degreased steel substrate of 40 mm × 50 mm × 1 mm without grit blasting. The coated specimen was clamped at one end using a sheet-bending machine to give a cantilever configuration. A force perpendicular to the surface of the specimen was applied at the free end of the sample to bend the specimen and the maximum angle before cracking or peel off from the substrate was recorded.

Wear performance was assessed using a reciprocating ball-on-flat machine with a stainless steel ball sliding against the flat coated surface. The stainless steel ball was 10 mm in diameter. Loads of 20 N or 40 N were applied to the steel ball, which slid at 60 cycles per minute over a track length of 24 mm on the flat-coated plate. Wear was evaluated by measuring the mean depth of the wear track on the polymer coating using a linear variable differential transducer (LVDT), connected to a computer for data collection and processing.

3. Results and discussion

3.1. UHMWPE coatings

3.1.1. Particle flow

A critical requirement for the thermal-spray deposition of dense coatings is that the feedstock particles should flow significantly on impact with the irregularities of the substrate or underlying splats. The flow characteristics of the UHMWPE were therefore studied by wipe testing, which consists of scanning the substrate very rapidly such that the impacts of individual splats can be observed as separated entities and not as the usual agglomerated deposit. The morphology of typical UHMWPE (Powder A, relative molecular weight: 6×10^6) particles produced in the wipe test is shown in Fig. 1a. It shows that the outer layer of a particle flows on impact but that its core undergoes little flow and exists as a protruding inner region. This is attributed to the low thermal conductivity of the UHMWPE, which results in a much lower temperature and therefore higher viscosity at the centre of the particle during its flight through the hot jet. For comparison, the particles from the same powder were also placed on a glass slide and heated in an oven at 200°C for 5 min. The morphologies of the oven-heated particles are given in Fig. 1b, which shows fully melted, homogeneous droplets. The homogeneity being due to the uniform heating resulting from the time being sufficient to reach thermal equilibrium. The more important observation, however, is that the droplets exhibit very little flow and show no tendency to wet the substrate. This contrasts with the situation in Fig. 1a in which the high impact velocity forces substantial flow. This behaviour implies that satisfactory deposition by electrostatic spraying is likely to be difficult but, on the other hand, that thermal spraying has potential for preparing dense UHMWPE coatings.

The particle flow in thermal spraying is generated by the stress σ at impact as the particle strikes the substrate at a velocity v and is given by:

$$\sigma = \frac{\rho v^2}{2} \tag{1}$$

where ρ is the density of the particle. If the particle is assumed to undergo viscous flow, it may be assumed to follow simple Newtonian behaviour:

$$\tau = \eta \frac{\partial v_x}{\partial y} \tag{2}$$

where τ is the shear stress, η is the viscosity, v_x is the velocity in the x direction (parallel to the surface) and y the dimension perpendicular to x. Equation 2 can be re-written in terms of the normal stress σ ($\tau = \sigma/2$) required to produce a strain ε in a particle of viscosity η and over a time interval of Δt:

$$\sigma = 2\eta\varepsilon/\Delta t \tag{3}$$

Equations 1–3 indicate that the degree of particle flow or strain is governed by the stress σ at impact and the melt viscosity of the polymer melt. A high stress is required for high-viscosity polymers to gain sufficient strain within a short time. In the case of the oven-heated particles, the stress deriving from gravity and surface tension was clearly (Fig. 1) much smaller than that of the impact stress in thermal spraying resulting in very little flow.

Fig. 2 gives the polished cross-section of a coating produced from Powder A. It shows a dense coating consisting of deformed particles/splats closely packed together. The boundaries of the particles can be seen clearly, which is quite different from low molecular-weight polymer coatings in which the splats fused together and the boundaries are not detectable. Examination of the morphologies of impinging particles of Powder A reveals the particle flow of the powder increased with increasing thermal power, suggesting that dense coatings should be obtainable using higher thermal power levels. However, the temperature

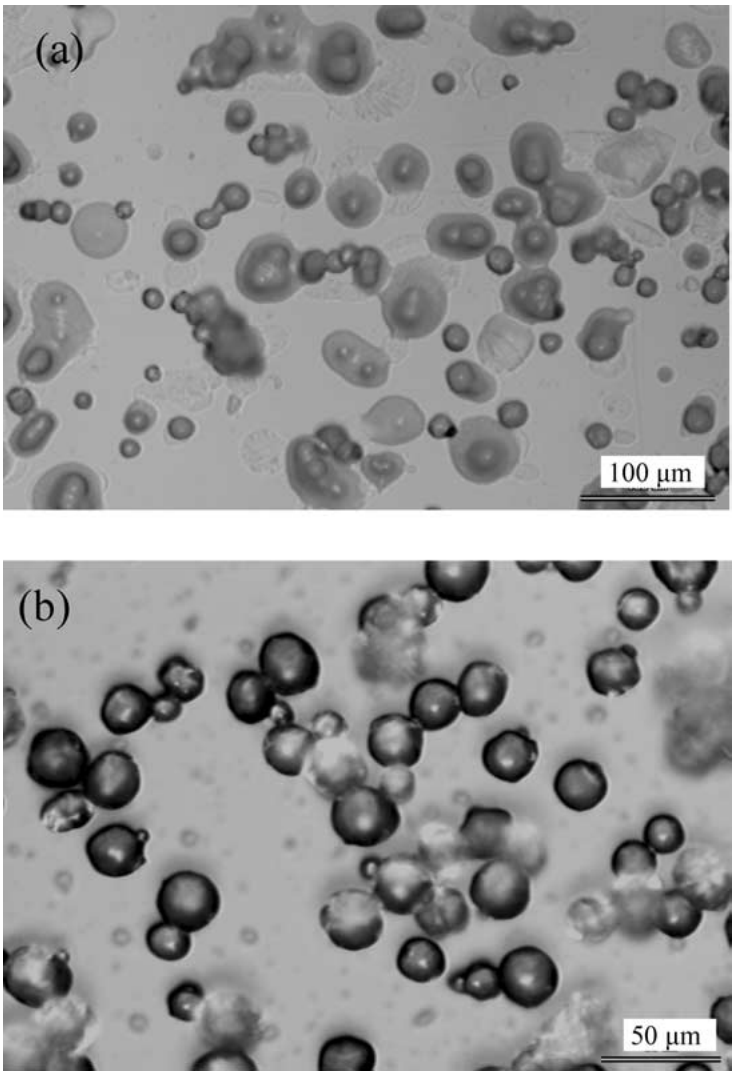

Figure 1 Morphologies of Powder A (relative molecular weight 6×10^6) particles from the wipe test: (a) thermal-spray deposited and (b) oven heated.

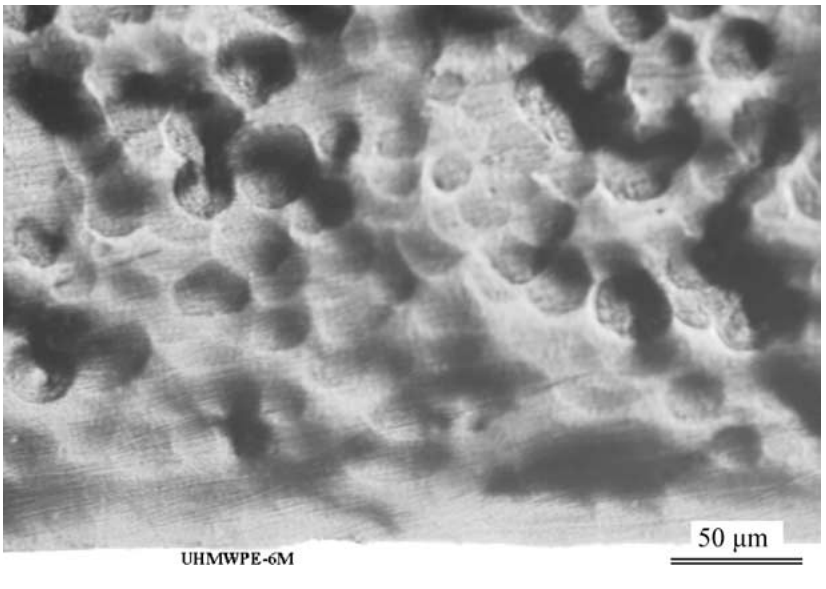

Figure 2 Polished cross-section of an UHMWPE coating produce from Powder A.

measurements on the deposits during deposition revealed that the high thermal-power levels caused excessive heating of the deposited layer and a serious risk of degradation. A compromise that gives the maximum degree of particle flow while avoiding degradation is required.

3.1.2. Molecular weight and particle size

A satisfactory particle flow was obtained from Powder A, which has a relative molecular weight of 6×10^6. However, sufficient particle flow under the same spray-deposition conditions could not be obtained with Powder B and satisfactory coatings could not be produced,

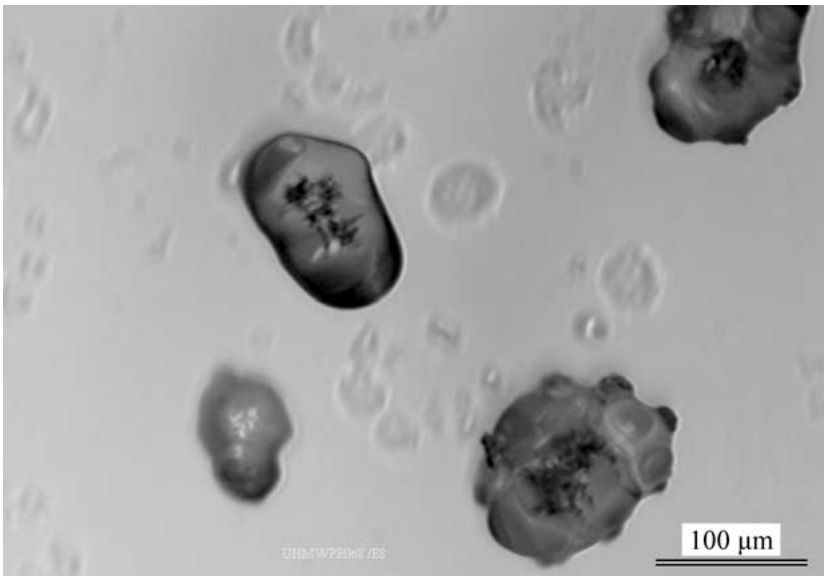

Figure 3 Morphologies of Powder B (relative molecular weight 2×10^6) particles produced by the wipe test.

even though it had a much lower molecular weight (2×10^6). Examination of the morphologies of impacted Powder B particles obtained from wipe test reveals that significant proportion of the particles bounced off the hard substrate during deposition. The traces of these particles are clearly observable in Fig. 3. The poor flow of the impinging particles resulted in insufficient contact area between the particles and substrate, which is required to retain the particles on the substrate surface. Attempts were made to improve the particle flow by increasing the thermal power of the flame but this did little to improve the flow and the coatings were unsatisfactory. In addition, some degradation of the UHMWPE occurred.

As shown in Table I, apart from the molecular weight, a distinct difference between Powder A and Powder B is the particle size: the average particle size (D_{50}) of Powder B is 120 μm, more than four times greater than that of Powder A ($D_{50} = 27$ μm). The particle size will affect the motion and heating of the particles in the hot gas jet. To understand the effect of particle sizes a computational model was developed to simulate the interaction between particles and the flame.

To simulate the temperature profile of the in-flight particles a computational model was developed using the following steps:

(1) Specify the temperature and velocity profile of the combustion flame. This can be controlled by varying the ratio between fuel gas and compressed air as well as changing the gun design. The temperature profile of the flame can be measured experimentally.

(2) Specify the properties of the combustion flame as a function of composition and temperature. The composition of the flame is defined by the ratio of the fuel gas to the oxidant (air in this study). The properties used in the calculation include specific heat (C_p), density (ρ), viscosity (η) and thermal conductivity (K). These properties as functions of temperature for individual gases (CO_2, O_2, N_2, and H_2O) can be found from the literature [10]. The properties of the flame are calculated using the addition law:

$$P_i = \sum_{j=1}^{n} x_j P_{i,j}$$

where, P_i is the property of the flame (C_p, ρ, η and K), x_j is the fraction of gas j and $P_{i,j}$ is the property of gas j.

(3) Calculate the velocities of the in-flight particles (v), which requires knowing the acceleration of particles as a function of position. The acceleration can be found from momentum equation:

$$m_p \frac{d\vec{U}_p}{dt} = \vec{F}_{dr} + \vec{F}_p + \vec{F}_{am} + \vec{F}_b \qquad (4)$$

where m_p is mass of the particle, $\vec{F}_{dr}$ the drag force, $\vec{F}_p$ is the force on the particle caused by pressure gradient. $\vec{F}_{am}$ is the force caused by the 'added-mass', which is required to accelerate the gas flow 'entrained' by the particle. $\vec{F}_b$ is the body force, in the present case, the gravitational force. In thermal spraying, the forces due to gravity and pressure gradient are very small, comparing with the drag force. They are neglected in the present study.

The drag force $\vec{F}_{dr}$ is given by:

$$\vec{F}_{dr} = \frac{1}{2} C_d \rho_g A_S |\vec{U} - \vec{U}_p| (\vec{U} - \vec{U}_p) \qquad (5)$$

where A_s is the surface area of the particle, C_d is the drag coefficient, which is a function of the particle Reynolds number Re_p, defined by:

$$Re_p = \rho_g |\vec{U} - \vec{U}_p| d_p / \mu_g \qquad (6)$$

The drag coefficient C_d at a given position is given

by:

$$
\begin{aligned}
C_d &= \frac{24}{\mathrm{Re}}, \quad \mathrm{Re} < 0.2 \\
C_d &= \frac{24}{\mathrm{Re}}\left(1 + \frac{3}{16}\mathrm{Re}\right), \quad 0.2 \le \mathrm{Re} \le 2 \\
C_d &= \frac{24}{\mathrm{Re}}(1 + 0.11\mathrm{Re}^{0.81}), \quad 2 \le \mathrm{Re} \le 21 \\
C_d &= \frac{24}{\mathrm{Re}}(1 + 0.189\mathrm{Re}^{0.632}), \quad 21 \le \mathrm{Re} \le 200
\end{aligned} \tag{7}
$$

For Reynolds numbers greater than 200, the drag coefficient was determined using experimental value given by Schlichting [11] and Hagen [10].

(4) Calculate the heat transfer coefficient (h) between the flame and in-flight particles.

$$\mathrm{Nu} = \frac{hd_p}{k_f} = 2 + 0.66\mathrm{Re}^{1/2}\mathrm{Pr}^{1/3} \tag{8}$$

where Nu is the Nusselt number and Pr is the Prandtl Number.

$$\mathrm{Pr} = \frac{C_{pf}\mu_f}{k_f} \tag{9}$$

where ρ_f, μ_f, k_f and C_{Pf} are the density, viscosity, thermal conductivity and specific heat of the gas jet respectively.

(5) Calculate the temperature distribution in the particles.

The heat transfer within the particles can be described by a special form of the general conduction equation in a spherical polar co-ordinate system:

$$\rho C_p \frac{\partial T}{\partial t} = \frac{1}{r^2}\frac{\partial}{\partial r}\left(kr^2\frac{\partial T}{\partial r}\right) \tag{10}$$

where r is the radial distance from the centre of the particle, T the temperature, t the time, and C_p, ρ and k the specific heat, density and thermal conductivity of the particles respectively. At the particle surface, the heat transfer coefficient (h) can be found from Equation 8:

$$h = (k_f/d_p)\mathrm{Nu} \tag{11}$$

(6) Calculate the new position based on the drag coefficient C_d.

(7) Repeat 2 to 6 to calculate temperature distribution of the particles at a distance z from nozzle exit.

Using the above computational model, the temperature profiles of the in-flight particles of UHMWPE Powder A and Powder B were calculated based on the measured temperature profile of the combustion flame. To simplify the calculation the following assumptions were made in the modelling:

(1) The particles were spherical.

(2) All the particles have same initial velocity before being injected to the flame (10 m/s)

(3) The properties of the particles and their volume remain constant. The melting enthalpy was taken as 291 kJ/kg [12].

The calculated temperature profiles for the powders with particle sizes of 27 and 120 μm are shown in Figs 4–5. The calculated results show that a much larger temperature difference between the surface and centre exists in large particles than in small particles. Since the polymer has a low thermal conductivity, the heat transfer from the hot jet to a polymer particle is controlled by the heat conduction from the surface of the particle to its core. The larger the particle, therefore, the greater the temperature difference that will be developed in the particle. Increasing the thermal power of the flame can only result in a rapid temperature rise in the surface layers of the particle. In the extreme, the surface of a particle may reach the polymer decomposition temperature while its centre still remains solid. When the large particles in Powder B strike the substrate, there is little effective flow due to the low core temperature resulting in insufficient contact area with the substrate and poor retention. The particle size is much smaller in Powder A ($D_{50} = 27$ μm). The temperature difference in the particles is much smaller and so full melting with extensive flow on impact is achieved.

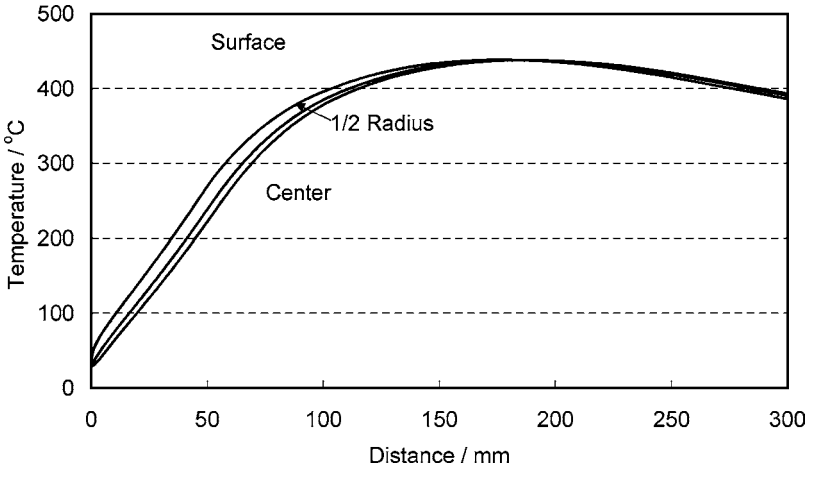

Figure 4 Temperature distribution of a 27 μm UHMWPE particle as a function of distance from nozzle exit.

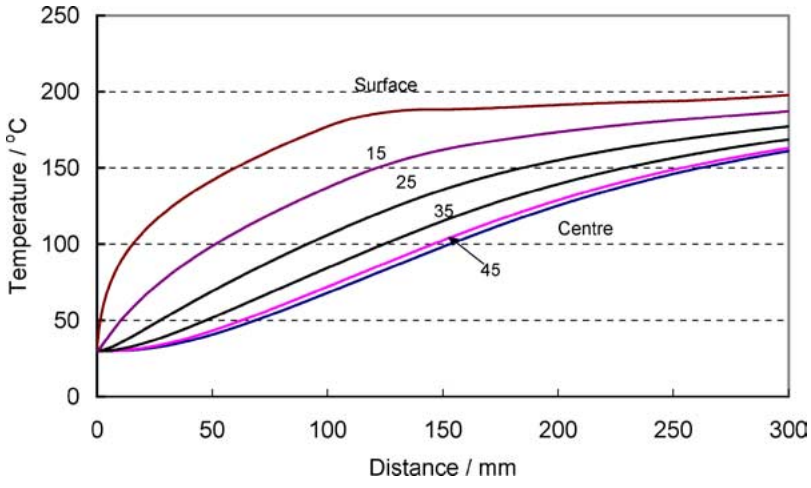

Figure 5 Temperature distribution of a 120 μm UHMWPE particle as a function of distance from nozzle exit. The numbers next to each line are the depth into the particle from its surface in micrometres.

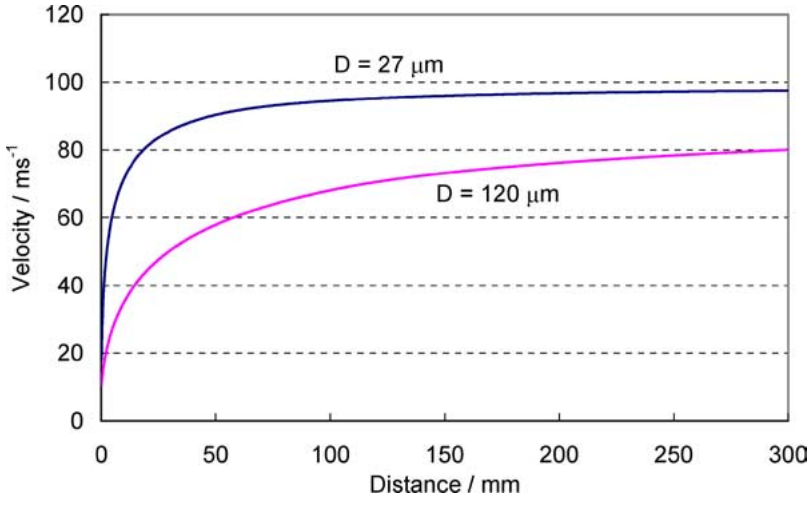

Figure 6 Velocities of 27 and 120 μm UHMWPE particles in the flame as a function of distance from nozzle exit.

Another factor affecting particle flow is the impact velocity. The particle velocities of powders with particle sizes 27 and 120 μm were calculated and the results are given in Fig. 6. This indicates that Powder A with average particle size of 27 μm would reach a velocity of 97 m/s whereas Powder B (120 μm) can only reach 80 m/s. The flow at impact of the particles in Powder B will therefore be expected to be significantly less than that of Powder A.

Deposition trials and particle morphological observations showed that the flow of similarly sized UHMWPE particles subjected to thermal spraying increased as the molecular weight decreased due to the influence of viscosity (Equation 3). These results suggests that for ultra-high molecular weight ($>10^6$) polymers, the particle size should be reduced to less than approximately 50 μm to ensure complete melting before impact with substrate. For lower molecular weight polymers, coarser powders may be sprayed owing to their lower viscosity.

The adhesion of UHMWPE coatings produced from Powder A deposited under various process parameters was evaluated using the pull-off technique. The coatings were deposited onto a 40 mm $\times$ 50 mm $\times$ 3 mm thick carbon steel substrate. The measured values of coating-adhesion were between 2 and 4 MPa. All failures occurred at the interface between the adhesive and the coating, indicating that the true adhesion and cohesive strengths were higher than the measured values.

3.2. UHMWPE-EAA duplex coatings

Experimental trials and theoretical analysis suggest that reducing the particle size of UHMWPE could promote the particle flow and improve the coating quality. However, reducing the particle size of UHMWPE requires high-energy grinding, which inevitably increases the processing cost. One approach to overcome the viscosity problem of UHMWPE would be to apply a bond layer between the UHMWPE and the steel substrate. The polymer used for the bond layer should: (a) exhibit good particle flow to enhance the intimate contact with the substrate; (b) contain a polar group in its molecular chain to promote bonding with the metallic substrate; (c) be compatible with the UHMWPE topcoat.

Ethylene acrylic acid (EAA) containing 6.5% acrylic acid was selected as a bond coat as its low molecular weight provides superior flow characteristics, its constituent electronegative oxygen atoms are highly polar and its molecular architecture is similar to and compatible with UHMWPE. The EAA was first sprayed onto the steel substrate. To ensure a reasonable particle

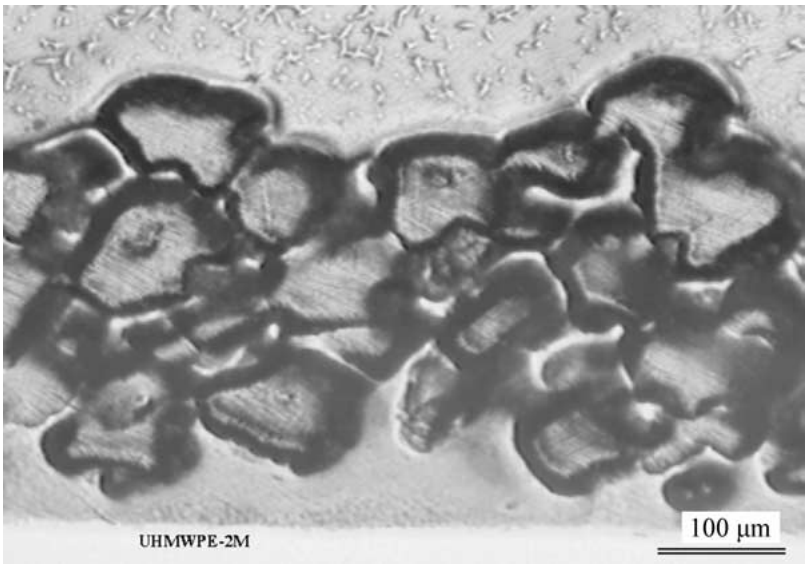

Figure 7 Polished cross-section of a UHMWPE (Powder B)-EAA double-layer coating. UHMWPE is dark phase in centre of field and EAA is light phase below.

flow, Powder B was sieved to less than 150 μm and then applied on top of the EAA bond coat. In this way, an UHMWPE-EAA double-layer coating was obtained. Microscopic examination revealed that the UHMWPE particles were embedded into the EAA layer at the UHMWPE/ EAA interface suggesting a sound bond between them (Fig. 7). However, it was observed that the UHMWPE deposit consisted of particles with many interstitial pores due to poor flow, particularly for the large particles. These partially molten particles adhered to one another but formed large interstitial pores.

The adhesion of the UHMWPE-EAA double-layer coating to the steel substrate was evaluated under the same conditions as described above. The measured results were in the range 3–5 MPa. The tensile failure occurred at the interface between the coating and the adhesive. The true adhesion strength of the coating to the substrate therefore could not be obtained. However, the test results and microscopic observations suggested that there was good bonding between the bond layer and the topcoat and between the bond layer and substrate. UHMWPE-EAA double-layer coated samples were also subjected to a bend test. The coating was deposited onto a 40 mm $\times$ 50 mm $\times$ 1.0 mm steel substrate without grit blasting. The top UHMWPE coating was observed to crack at a bend angle of 20 degrees, but no cracks were observed to penetrate into the EAA bond layer at this angle. This indicates that the UHMWPE coating was relatively brittle due to the high fraction of interstitial pores.

3.3. UHMWPE-EAA composite coatings

Although the adhesion strength of the UHMWPE coatings produced by larger particle sizes was improved by applying a bond coat, the cohesive strength and ductility of the coatings were not satisfactory and the porosity was high. An UHMWPE-EAA composite was therefore developed in order to improve the particle flow during deposition and improve the cohesive and adhesive strength and ductility of the UHMWPE coating. In order to obtain a satisfactory composite, the UHMWPE-EAA system was manufactured by co-extrusion using 50% Powder B and 50% EAA. The extrudate was then ground to powder and the resulting particle size distribution is given in Table I.

The particle flow of the composite particles under different spray conditions was investigated using wipe testing. The results showed that the composite powder exhibited much better particle flow (Fig. 8) and higher deposition efficiency than pure UHMWPE particles (Fig. 3). The powder was then used to deposit coatings under various conditions. The temperature of the polymer coating during deposition was monitored and recorded in order to understand the process-structure-property relationships. It was observed that raising the thermal power from 5 to 10 kW increased the average temperature of the coating during deposition from 200 to 350°C. This is likely to have a major effect on coating characteristics and properties.

A microstructural examination of the UHMWPE-EAA composite coatings showed that they were much denser than the UHMWPE-EAA double-layered coatings (Fig. 9). It also revealed that the composite coating consisted of two phases: large poorly flowed particles embedded within a well-melted matrix (Fig. 9a). Microhardness tests showed that the large partially molten particles had a higher hardness 4.8 HV (10 g load for 5 s) than that of the molten matrix phase 1.7 HV (10 g, 5 s) suggesting that the partially molten particles may have a higher UHMWPE content than the molten matrix phase.

The adhesion of the UHMWPE-EAA composite coatings deposited at different thermal power levels onto the steel substrate was evaluated using the pull-off technique. The measured values were 5–6 MPa, which were higher than those of the double-layer coatings (3–5 MPa). The UHMWPE-EAA composite coatings showed great improvement in ductility. These coatings

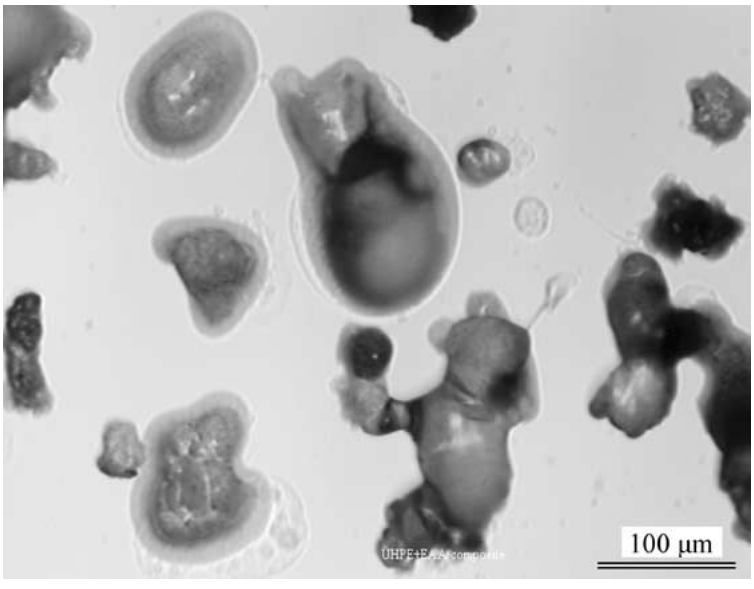

Figure 8 Morphologies of UHMWPE (Powder B)-EAA particles produced by the wipe test.

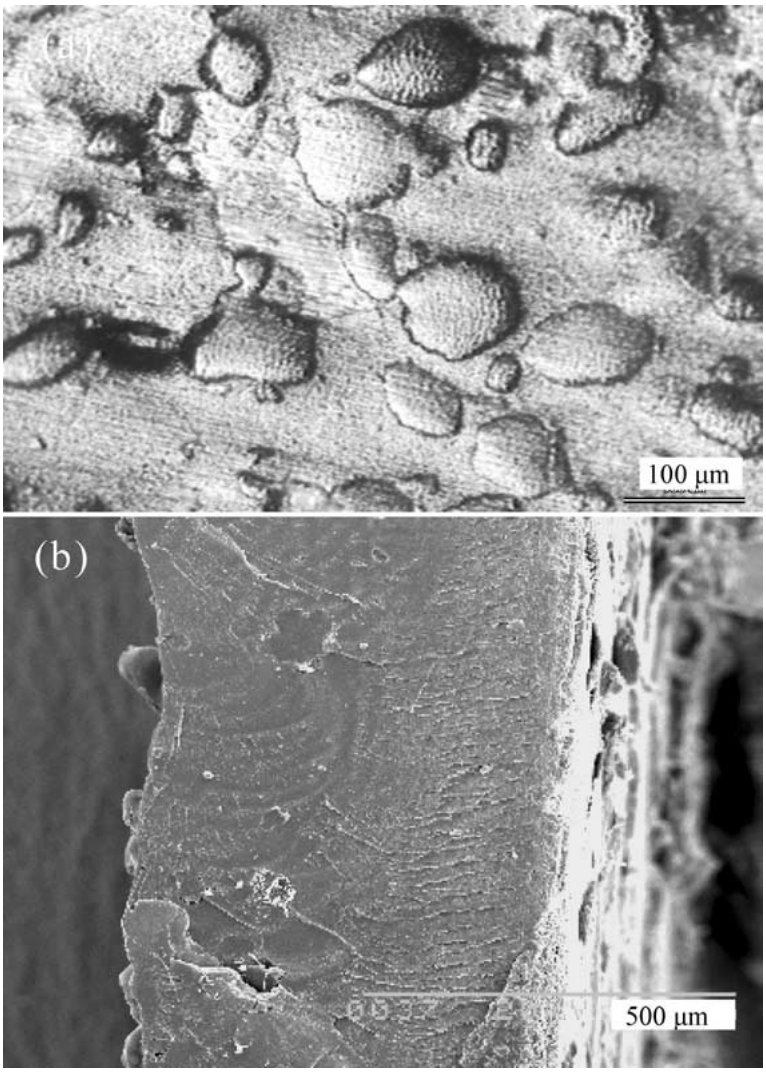

Figure 9 Thermally sprayed UHMWPE (Powder B)-50%EAA coatings: (a) polished cross-sectional and (b) fracture surface (SEM).

could be bent to 90° without cracking, while the topcoat of the UHMWPE-EAA double-layered coatings started cracking at 20°. The reduced interstitial pores within the UHMWPE-EAA composite coatings, as shown in Fig. 9, played an important role in the improvement of the cohesion of the coating and hence the ductility.

3.4. Wear behaviour

Fig. 10 gives the wear curves of UHMWPE-EAA composite coatings produced with flames of various thermal power levels. It shows an initial period of rapid wear or running-in over the first 500 cycles followed by a more gradual steady-state wear period. Fig. 11 was plotted

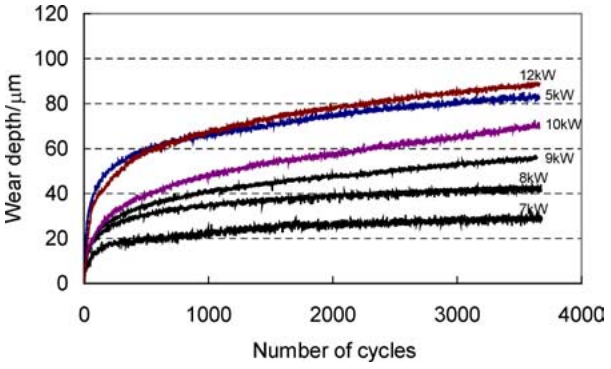

Figure 10 Wear curves of UHMWPE (Powder B)-EAA composite coatings deposited under various thermal powers. Load: 20N.

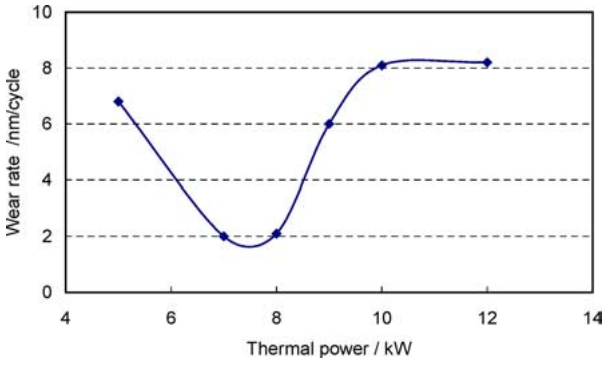

Figure 11 The influence of thermal power of the flame on wear rate of the UHMWPE-EAA composite coatings.

using the data from Fig. 10 and shows the influence of the thermal power on the wear rate in the steady-state regime of these UHMWPE-EAA composite coatings. This indicates an optimum thermal power of 7–8 kW corresponding to a minimum wear rate. The temperature of the coating was found to increase substantially with increasing thermal power suggesting that the deteriorating wear performance at high powers was caused by polymer degradation. The poor wear performance at low power levels is attributed to inadequate heating of feedstock particles in the flame, inferior particle flow and consequent voidage in the coating. The optimal power value will depend on the particular set of conditions applied during deposition, because other conditions (e.g., spray distance, torch scanning speed) will also affect the structure of the coating.

Fig. 12 compares the wear performance of the coatings of pure EAA, the UHMWPE-EAA double layer and the UHMWPE-EAA composites. The coatings were produced at their optimum thermal power levels and wear tested under a load of 40 N against a stainless steel ball. The results show that UHMWPE coatings provide a much better wear resistance than those of EAA. There was little difference between the steady-state wear rates of the UHMWPE-EAA double-layer and composite coatings. However, the composite coating had a higher ductility in the bend tests and so is expected to offer the greater potential for general engineering applications.

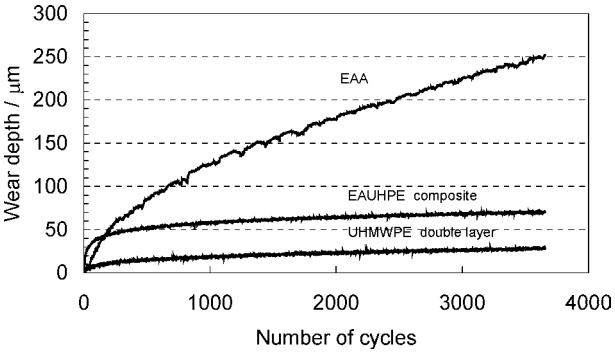

Figure 12 Wear curves of EAA, UHMWPE-EAA composite and UHMWPE-EAA double-layer coatings. Load: 40N.

4. Conclusions

(1) UHMWPE coatings with relative molecular weights up to 6 million were produced by combustion flame spraying. The deposition of pure UHMWPE was sensitive to the processing conditions and powder characteristics. A process window in terms of flame feedstock power and particle size is required for deposition.

(2) The coatings produced with UHMWPE were relatively brittle. The use of a bond layer improved the adhesion but provided little improvement in the ductility of the coatings.

(3) The use of a low molecular weight EAA as a matrix phase for UHMWPE provided substantial gains in the adhesion and ductility of the coating while maintaining the wear performance.

Acknowledgements

The authors would like to thank the European Commission for sponsoring the research and for permission to publish the results.

References

1. T. S. BARRETT, G. W. STACHOWIAK and A. W. BATCHELOR, *Wear* **153** (1992) 331.
2. C. M. POOLEY and D. TABOR, *Proc. R. Soc. Lond., Ser.* A **329** (1972) 251.
3. J. K. A. AMUZU, B. J. BRISCOE and D. TABOR, in "Advances in Tribology" (Institute of Mechanical Engineers, London, 1978) p. 59.
4. K. MARCUSAND and C. ALLEN, *Wear* **178** (1994) 17.
5. J. R. ATKINSON, K. J. BROWN and D. DOWSON, *J. Lubrication Technol.* **100** (1978) 208.
6. *Idem., ibid.* **104** (1982) 17.
7. K. MARCUS, A. BALL and C. ALLEN, *Wear* **151** (1991) 323.
8. R. M. ROSE, H. U. GOLDFARB, E. ELLIS and A. M. CRUGNOLA, *ibid.* **92** (1983) 99.
9. A. WANG, D. C. SUN, S. S. YAU, B. EDWARDS, M. SOKOL, A. ESSNER, Y. K. POLINENI, C. STARK and J. H. DUMBLETON, *ibid.* **203/204** (1997) 230.
10. K. D. HAGEN, "Heat Transfer with Applications" (Pentice-Hall International (UK) Limited, London, 1999).
11. H. SCHLICHTING, "Boundary Layer Theory", 7th ed. (McGraw-Hill, New York, 1979).
12. S. H. SPIEGELBERG, "Analytical Techniques for Assessing the Effects of Radiation on UHMWPE," Cambridge Polymer Group, Application Note 008, 2001.

Received 28 January
and accepted 31 August 2004